2018 IEEE Intelligent Vehicles Symposium (IV)
Changshu, Suzhou, China, June 26-30, 2018

Efficient Rectangle Fitting of Sparse Laser Data for Robust On-Road Object Detection

Shuai Yang, Zhaohong Xiang, Jin Wu, Xiao Wang, Hongbin Sun*, Jinming Xin and Nanning Zheng

Abstract— **On-road object detection is one of the most important tasks for the autonomous driving of intelligent vehicle. Nevertheless, the previous methods based on 2D LIDAR sensor only focus on the detection of vehicles, and show severe limitations on the detection of other objects. Accordingly, this paper proposes an on-road object detection method, which employs rectangle fitting and concavity determination to improve the robustness of object detection. The proposed approaches are extensively evaluated by using the sparse laser data collected by 2D LIDAR from real traffic environment. Experimental results demonstrate that the proposed rectangle fitting outperforms the previous approaches in terms of both detection accuracy and computational efficiency.**

I. Introduction

Autonomous driving technology is rapidly growing to meet the needs of road safety and transportation efficiency [1]. One of the most important aspects in autonomous driving technology is the reliable environment perception [2], [3]. Environment perception is dedicated to detect and track various static and moving objects from road environment, and may further perform some inferences such as vehicle behavior and scene understanding. On-road object detection is the first step of environment perception. In order to thoroughly understand the environment, intelligent vehicle needs to detect not only the existence of objects, but also the poses of them. Based on the environment perception, intelligent vehicle can plan right path while avoiding collision with moving vehicles, pedestrians and other on-road objects [4].

A variety of sensing modalities have become available for on-road obstacle detection, including Radar, LIDAR, and camera [5]. Radar uses the signal of radio waves to determine the range, angle, or velocity of objects. Although Radar is consistent in different illumination and weather conditions, its measurements are usually noisy and need to be filtered extensively. LIDAR utilizes pulsed laser light to detect the distance to objects. Compared with Radar, LIDAR provides a much wider field-of-view and cleaner measurements. Vision sensors provide a rich data source and a wide field of view, from which additional information and context can be surmised. Nevertheless, the major drawbacks to vision-based object detection are very sensitive to light and weather conditions. Therefore, vehicle-mounted LIDAR sensing is emerging as a leading technology for research-grade intelligent vehicles.

There are generally two kinds of vehicle-mounted LIDAR, i.e. 2D and 3D LIDAR. Compared with 2D LIDAR, 3D LIDAR (e.g. the Velodyne HDL-64) can provide high-definition 3D point clouds and hence has been widely used to drivable-region detection, obstacle detection and tracking, map building and localization, and so forth. However, the high-definition 3D LIDAR sensors are very expensive and still cannot be commonly used on production vehicles. Therefore, 2D LIDAR that provides sparse 2D point cloud data has also attracted much attention. Several previous works have explored to use sparse laser data for vehicle detection [2], [6], [7] or object classification [8], [9]. In these designs, vehicular shape model fitting is one of the key techniques, as it provides feeds for vehicle detection and tracking. Therefore, a variety of vehicle shape models and their fitting approaches have been explored [6]–[8], [10].

This paper focuses on on-road object detection and pose estimation using sparse 2D laser. As all the previously proposed fitting approaches are only designed for vehicle detection, they show severe limitations and deficiencies especially when being used to detect other objects besides vehicle. Accordingly, this paper proposes a robust and efficient on-road object detection method based on 2D LIDAR sensor. Compared with previous methods, we make the following three major contributions in this paper.

- The proposed concavity determination approach and its corresponding operations are added into the object detection flow to address the issue incurred by concave objects;
- Based on the rectangular model assumption, a rectangle fitting approach is proposed to improve the robustness of on-road object detection;
- We further propose a contour aggregation criterion to effectively evaluate the fitting performance and find the best-fit rectangle bounding box.

Experimental results demonstrate the effectiveness and efficiency of the proposed object detection and rectangle fitting approach. Compared with previous L-shape fitting [7], the proposed rectangle fitting improves the

This work was supported partly by National Key R&D Program of China (No. 2017YFC0803907), National Natural Science Foundation of China (No. 61790563), and Joint Foundation of Ministry of Education of China (No. 6141A02033303)

The authors are with the Institute of Artificial Intelligence and Robotics, Xi'an Jiaotong University, Xi'an, Shaanxi, 710049 P.R. China
*Corresponding author: Hongbin Sun, hsun@mail.xjtu.edu.cn

average normalized unoverlapped area and orientation error by up to 0.07 and 3.52° respectively. The average computation time of the proposed rectangle fitting is also 32% lower than that of L-shape fitting.

II. Background and Motivation

As shown in Fig. 1, LIDAR system is based on the Time of Flight (ToF) method. A LIDAR sensor emits a short laser pulse to measure the time that elapses until the laser pulse is reflected by an object and subsequently received by the sensor. Due to the constant propagation of light, the distance to the reflecting object can be calculated by measuring the time between the emission, the reflection, and the subsequent receipt by the sensor. In 2D LIDAR system, LIDAR sensor emits a sequence of short laser pulses in different directions and receives them again. 2D LIDAR may use multiple measurement layers where multiple beams scan the environment at different height. This scanning by the laser beams enables a 2D representation of the environment which is suitable for environmental perception in traffic scenarios.

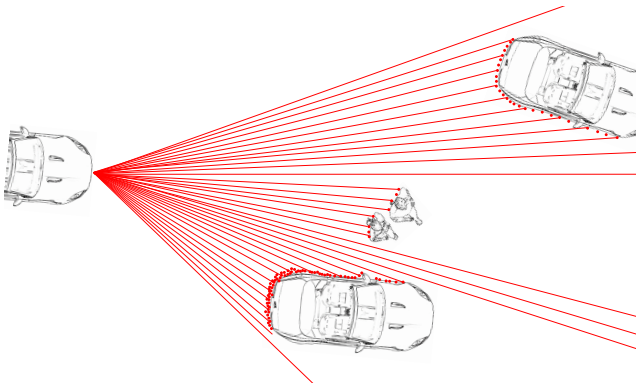

Fig. 1: Schematic diagram of 2D LIDAR.

In general, the sparse laser data from 2D LIDAR is firstly segmented into clusters. These clusters typically correspond to vehicles, bicycles, or pedestrians, and can be used to object detection. Nevertheless, compared with dense laser data from high-definition 3D LIDAR, the sparse laser data poses major challenges for object detection task. With 2D LIDAR sensing, we can only detect parts of the object's contour that are facing towards the sensor. In this case, previous works only exploit the sparse laser data for vehicle detection. To address the difficulty of sparse 2D laser data, a vehicular shape model which abstracts geometric features of the desired target is widely adopted for feature extraction and vehicle pose estimation. The commonly used vehicular shape models include L shape [6], boxes [8], and two perpendicular lines [9]. The features for target tracking can be easily extracted from the vehicular shape model fitted by the incomplete contour.

Vehicular shape model and fitting algorithms are critical to the vehicle detection and tracking based on sparse laser data. A variety of related methods have been proposed. [8] uses rectangular model and conducts both a line fitting and a right-angle corner fitting to mitigate the occlusion problem. However, not all clusters contain evident corner point. This significantly limits the application of the method. [9] applies Principal Component Analysis (PCA) on laser points to detect the two orthogonal edges of vehicle. [10] generates a height map by using height threshold and extracts only parallel edges to fit a rectangle model. [6] splites the point cloud into two mutually exclusive sets and fits them with two orthogonal lines respectively. In [7], a L-shape model fitting is proposed to achieve an optimal vehicle detection and pose estimation. The L-shape fitting approach does not depend on the scan sequence or ordering information, and is also computationally efficient and easy to implement.

Although the L-shape fitting approach in [7] has demonstrated its effectiveness in a variety of situations, but there are still some limitations especially when using this model to detect other objects besides vehicle. Fig. 2 (c) - (h) show three cases that L-shape fitting fails to correctly detect the objects.

- Fig. 2 (c) and (d) show a vehicle whose point clouds from 2D LIDAR is U-shape or L-shape. In this case, L-shape fitting is influenced by two edges of U-shape and results in an incorrect object detection that the orientation of the rectangle bounding box is wrong.
- Fig. 2 (e) and (f) show a object whose shape is irregular. As a matter of fact, many on-road objects such as bicycles, pedestrians or other obstacles are in irregular shape. For these kind of objects, L-shape fitting certainly results in incorrect detection. In this figure, the orientation error of rectangle bounding box is considerable that it will significantly influence the following path plan.
- Fig. 2 (g) and (h) show a special case that the object is in concave shape. In this paper, this kind of object is referred to as concave object. For the case of concave object, the simple use of L-shape fitting and rectangle bounding box will result in a mistake that a large percentage of road area will be occupied by the rectangle bounding box and the vehicle has to stop unexpectedly.

The deficiency of L-shape fitting motivates us to use other shape model and explore more robust fitting algorithm for on-road obstacle detection.

III. Proposed On-Road Obstacle Detection

A. Overall Flow

Fig. 3 illustrates the overall flow of the proposed on-road object detection based on sparse laser data. Similar to previous works on vehicle detection, sparse laser data from 2D LIDAR is firstly transformed from laser coordinate to the coordinate of vehicle where LIDAR is mounted on, Then, these points are segmented

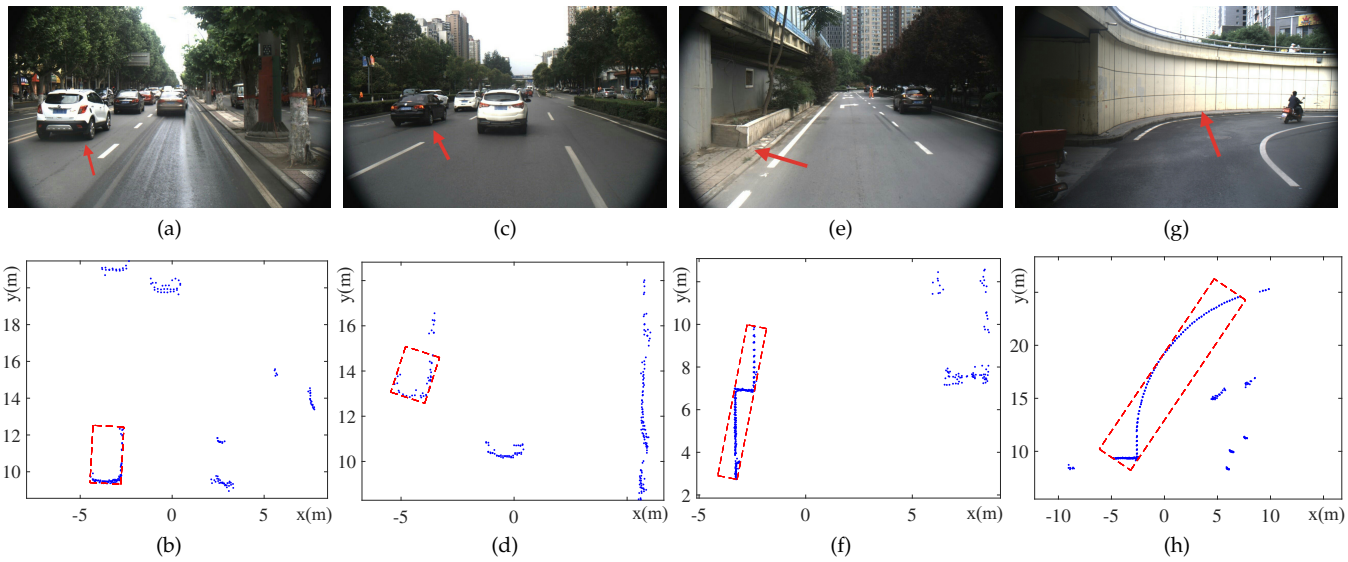

Fig. 2: Four examples when using L-shape fitting in on-road obstacle detection.

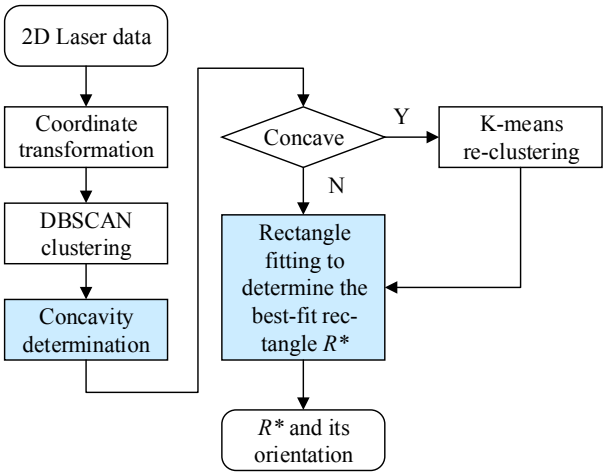

Fig. 3: Overall flow of the proposed on-road object detection method.

into each cluster. In the proposed method, DBSCAN algorithm [11] is employed for laser point clustering. DBSCAN is a classic density-based data clustering algorithm that has the excellent ability of discovering all shapes of clusters. Moreover, as this work focuses on the processing sparse laser data, DBSCAN can also satisfy the real-time requirement as well. In this paper, we take preprocessing and clustering as given and focus solely on the subsequent steps. Two substantial differences between the proposed object detection and previous vehicle detection methods are: (1) Concavity determination and the corresponding operations are added to address the issue incurred by concave object; (2) A rectangle fitting approach is proposed to improve the robustness of on-road object detection.

The issue incurred by concave object is mainly because that the use of a single 'big' rectangle bounding box occupies large road area. A feasible solution is to break the big concave cluster into several smaller clusters, whose boxes will not occupy too much road area (no need to make sure each of these small cluster are convex). Accordingly, we propose to firstly determine the concavity of each detected cluster, and break the cluster into a group of smaller clusters in the case of concave cluster. K-means method is employed for the re-clustering operation, as K-means is a supervised clustering algorithm and can re-clustering the cluster as the defined number k. The clusters after K-means re-clustering can be processed by the following shape model fitting as other ordinary clusters.

To improve the robustness of object detection especially for objects with irregular shape, we further propose a rectangle fitting approach based on the rectangle model assumption of objects. As rectangle bounding box is finally used for each detected object, we can achieve better results by the direct use of rectangle model. Then, optimal object detection and pose estimation can be achieved by using efficient rectangle fitting approach. We presents the detail of concavity determination and rectangle fitting in the following subsections.

B. Concavity Determination

Concavity determination is critical to the correct processing of concave object. The algorithm employed in this work should not only be efficient enough to meet the real-time requirement, but also have the ability to distinguish the concavity of the cluster precisely. The overall concavity determination algorithm is presented in Algorithm 1.

The basic idea of concavity determination is very simple. As shown in Fig. 4 (a), we draw a straight line (red dotted line) to connect the first and last points after the cluster is sorted according to the polar angle of each

point in it. The straight line l separates the coordinate into two sides. For a concave cluster, the majority of points in the cluster should locate on the opposite side to the origin of (x,y) coordinate system, and these points should be in concave shape. While for a convex cluster, the majority of points in the cluster should locate on the same side as the origin of coordinate, and these points should be in convex shape. Therefore, we determine an object as concave object when its cluster satisfy the following two conditions simultaneously.

- The points set S that locate on the opposite side to the origin of coordinate account for more than $T\%$ of the cluster.
- The function $g(x')$ generated by the points set S satisfies a concave function.

Algorithm 1 Concavity Determination

Input: Points of one cluster: $p = [x, y]^T \in R^{2*n}$
Output: Concavity of the cluster

```
Compute the polar angle θ for every point in p
p_1, p_end ← arg min θ, arg max θ
θ_0 ← the angle of inclination of line l defined by p_1, p_end
(p', O') ← ConvertToNewCoor(p, origin point, θ_0)
d ← the y value of concave part of p'
L_1, L_2 ← the length of concave and convex part on x' axis
Set t ∈ [0, 1]
if L_1/(L_1 + L_2)) ≥ 0.5 then
    if d(Round(t*1+(1−t)*end))< t*d(1)+(1−t)*d(end) then
        Marks the cluster as a concave one.
    end if
end if
```

The definition of $g(x')$ is as follows. We set the intersection point of line l and the cluster as the origin point O of a new (x′,y′) coordinate system whose x-axis x' coincides with the line l, as shown in Fig. 4 (a). Then, $g(x')$ is defined as the distance from x′ axis to the points in the cluster. $g(x')$ should satisfy a concave function: suppose X' is the definition domain of $g(x')$, $g(x')$ is concave if $\forall x'_1, x'_2 \in X'$, $t \in (0, 1)$

$$g(tx'_1 + (1-t)x'_2) < tg(x'_1) + (1-t)g(x'_2) \qquad (1)$$

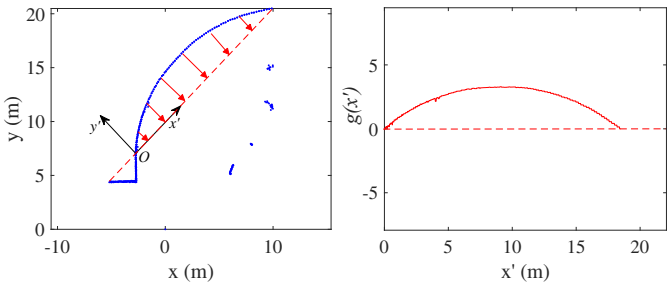

(a) (b)

Fig. 4: Concavity Determination

C. Rectangle Fitting

The benefit of using rectangle fitting to improve the robustness of object detection is obvious. The key to the proposed rectangle fitting is to find a suitable criterion to evaluate the fitting performance and choose the best-fit rectangle. Several criteria have been proposed previously in L-shape fitting for vehicle detection. X. Shen et al. [6] directly uses the $l2$ norm of the Euclidean distances between cluster points to the corresponding line. X. Zhang et al. [7] considered three criteria for selecting the rectangle, i.e. rectangle area minimization, points-to-edges closeness maximization, and points-to-edges squared error minimization. According to the evaluation in [7], the criterion of points-to-edges squared error minimization gives the best fitting performance. Nevertheless, through the extensive evaluation, we find that the previously proposed criteria are deficient and can be significantly improved.

We select 1360 clusters collected from urban roads and manually label the best-fit rectangle bounding box for each cluster. Then, we calculate the distance from each point to its nearest edge of the bounding rectangle, and generate the distribution histogram, as shown in Fig. 5 (a). We can see that the percentage of points with the closest distance is much smaller than what we expect. An example of cluster fitting is further shown in Fig. 5 (b), which confirms that the histogram results are actually reasonable. As the laser points are reflected by the contour of the object, they should aggregate to the contour edge, not the bounding edge. Hence, the extreme point in the histogram is actually around the contour edge. This may be the reason that the criterion of points-to-edges (bounding edges) closeness maximization shows relatively poor fitting performance. Therefore, the optimal criterion may evaluate how well the points aggregate to the contour edge.

We accordingly propose a ConTour AggreGation (CTAG) criterion to find the best-fit bounding rectangle. The proposed CTAG criterion can appropriately evaluate the degree of point aggregation near the contour.

The distribution histogram of the distances from points to contour edges (the position of the extreme points in Fig. 5 (a)) is generated and illustrated in Fig. 6 (a). We then fit the distribution histogram with a function and use the function to evaluate the degree of point aggregation near the contour. In this paper, the repulsive potential gradient function from the artificial potential field method [12] is utilized as the approximation of the distribution histogram to form the criterion, as shown in Fig 6 (c). The repulsive potential gradient function is defined as follows.

$$f(d) = \begin{cases} \eta(\frac{1}{D*} - \frac{1}{d})\frac{1}{d^k}, & d \le D* \\ 0, & d > D* \end{cases} \qquad (2)$$

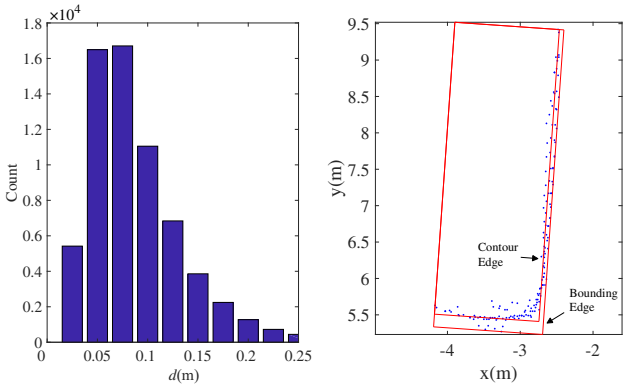

(a) (b)

Fig. 5: Distribution histogram of the distances from points to bounding edges.

Where, η is the repulsive gain factor, and k is 0.5. $D*$ is the threshold of effective distance. Denote the points of a cluster as $p = \{(x_i, y_i)|i = 1, 2, \cdots, n\}$ in 2D laser (x, y) coordinate. Alg. 2 shows all the detail steps of the CTAG criterion. Function *Rasterization* on line 2 is to project all the cluster points to a grid (the grid length is 0.05m).

Algorithm 2 CTAGCriterion(p', B)

Input: p', B
Output: Criterion value of rectangle B: $Criterion$
1: $B \leftarrow$ EdgesPositionAdjustment(B)
2: $q \leftarrow$ Rasterization(p'), $Q \leftarrow$ Rasterization(B)
3: $Criterion \leftarrow 0$
4: **for** i=1 **do** to sizeof(q) step 1
5: Take the i^{th} point of q: (x_i, y_i)
6: $dis \leftarrow$ MinDistance(x_i, y_i, Q)
7: **if** $dis > D_0 \&\& dis > 0$ **then**
8: $Criterion \leftarrow Criterion + \eta(1/dis - 1/D_0) * (1/dis^k)$
9: **end if**
10: **if** dis == 0 **then**
11: $Criterion++$
12: **end if**
13: **end for**
14: $Criterion \leftarrow \overline{Criterion}$

By using the CTAG criterion, we can firstly find the contour and optimize the θ of the rectangular bounding box to find a best-fit one for the cluster. θ is defined as the angle between one edge of the rectangle and the y axis. Then the approach can be formulated as follows,

$$\begin{aligned} \max_{A,B,C,D,\theta} \quad & \sum_{a\in A} f(|\cos\theta x_a + \sin\theta y_a - c_1|) \\ & + \sum_{b\in B} f(|\cos\theta x_b + \sin\theta y_b - c_2|) \\ & + \sum_{c\in C} f(|-\sin\theta x_c + \cos\theta y_c - c_3|) \\ & + \sum_{d\in D} f(|-\sin\theta x_d + \cos\theta y_d - c_4|) \\ s.t. \quad & \begin{cases} A \cup B \cup C \cup D = \{(x_i', y_i')\} \\ 0° \le \theta < 90° \quad (i = 1, 2, \cdots, n) \end{cases} \end{aligned} \tag{3}$$

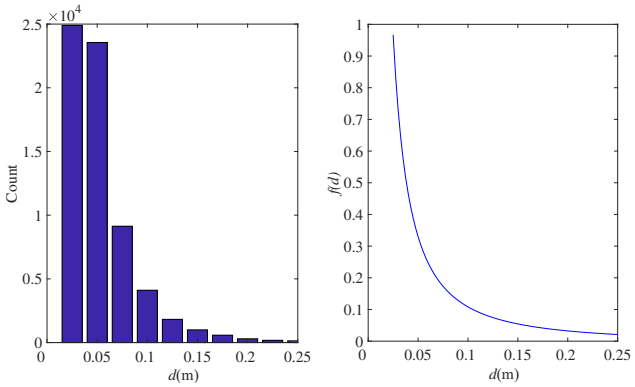

(a) (b)

Fig. 6: Distribution histogram of the distances from points to bounding edges and the repulsive potential gradient function.

Where, c_1-c_4 are locations of four contour or bounding edges. The points of cluster are splitted into four subsets A, B, C and D according to their distances to four bounding edges. Equation (3) is designed to find the optimal parameter θ by maximize the criterion value. We can apply an optimization search to obtain the best-fit rectangle by iteratively calculating the criterion value for the bounding rectangle of each angle θ and retain the one with largest criterion value, as demonstrated in Alg. 3.

Algorithm 3 Rectangle Fitting

Input: Points of one cluster: $p = [x, y]^T \in R^{2*n}$
Output: Four vertexes of the best-fit rectangle: $B_{best} = [\mathbf{X}, \mathbf{Y}]^T$
1: $Score \leftarrow 0$, $Criteria \leftarrow 0$
2: $Flag \leftarrow false$
3: **for** $\theta = 0$ to $\pi/2$ step π/m **do**
4: $p' \leftarrow$ Rotate p by $R(\theta)$
5: $B \leftarrow$ Four vertices of the bounding box of p'
6: **if** It is the first loop **then**
7: $Criteria \leftarrow$ CTAGCriterion(p', B)
8: **else**
9: $Score \leftarrow$CTAGCriterion(p', B) $-Criteria) - \delta$ // δ is set to avoid little noise of $Score$
10: **end if**
11: **if** $Score > 0$ **then**
12: $Criteria \leftarrow$CTAGCriterion(p', B)
13: $B_{best} \leftarrow B, R_{best} \leftarrow R$, $Flag \leftarrow true$
14: **end if**
15: **end for**
16: $B_{best} \leftarrow Flag * (R_{best}^{-1} * B_{best}) + !Flag * (R^{-1} * B)$

Compared with L-shape fitting who splits the cluster points into two subsets P, Q respectively, we take the all four bounding edges into consideration and split the points into four subsets. Seemingly the computation time doubles due to the increase of considered edges. Actually, the computational complexity remains essentially unchanged, because both of the two approaches use the same number of points in the cluster. But the step to find two boundaries which are closer to the

laser points by L2 norm [7] is eliminated in proposed approach, which has led to a reduction in computational complexity.

IV. Experimental Results

A. Experimental Setup

As shown in Fig. 7, all the object detection experiments are conducted on "Discovery" autonomous vehicle research platform developed by Xi'an Jiaotong University (XJTU). "Discovery" won the China Intelligent Vehicle Future Challenge (IVFC) 2017, where the performance and robustness of the proposed object detection and rectangle fitting approach has been extensively verified.

Fig. 7: XJTU autonomous vehicle research platform "Discovery".

The laser data used in the experiments are collected by one Ibeo LUX-8L which is mounted in front of "Discovery". Ibeo LUX-8L is a 2D LIDAR which can provide eight layers of range scan. The laser sensor works at the scan frequency of 6.25Hz in obstacle detection mode. To evaluate the correctness and efficiency of the proposed algorithms, approximately 40,000 laser scans were collected on urban roads. These laser scans are segmented frame by frame into around 110,000 clusters in total. All the laser scans and clusters are used to test the computational efficiency of the proposed rectangle fitting and obstacle detection. In addition, to test the correctness of the proposed rectangle fitting approach, we select a dataset of 411 clusters of points, including 104 vehicles and 307 other objects. The best-fit rectangle bounding box and its orientation of each cluster in the dataset is are manually labeled at resolution 1°.

B. Object Detection Results

Using the manually labeled dataset, we compared the proposed rectangle fitting approach with two reference approaches, i.e. PCA [9] and L-shape fitting [7]. In particular, we employ variance criterion in L-shape fitting, as it has the best fitting performance according to the evaluation in [7]. Moreover, we further evaluate the proposed rectangle fitting with two fitting criterions, i.e. variance criterion and the proposed CTAG criterion. These two approaches are referred to as rectangle fitting with variance (Rec-var) and rectangle fitting with CTAG (Rec-CTAG) respectively.

In addition, we use two metrics, i.e. normalized unoverlapped area (NUA) and orientation error, to evaluate the performance of the four approaches. Normalized unoverlapped area is defined as the differences between the ground truth rectangle bounding box and the rectangle bounding boxes generated by different approaches. In detail, it is defined as equation (4).

$$NUA = \frac{(A_{gt} - A_{ol}) + (A_{ap} - A_{ol})}{A_{gt}} \tag{4}$$

Where, A_{gt} represents the area of ground truth rectangle bounding box and A_{ap} represents the area of rectangle bounding box generated by different approaches, and A_{ol} represents the overlapped area of the two rectangle bounding boxes. Orientation error is defined as the orientation difference between the ground truth and generated rectangle bounding boxes.

The comparison of the histograms of two metrics are illustrated in Fig. 8 and Fig. 9 respectively. The figures clearly demonstrate that the proposed rectangle fitting approach with aggregation criterion significantly outperforms the other approaches in terms of both normalized unoverlapped area and orientation error. We also calculate the mean and standard deviation (STD) for the normalized unoverlapped area and absolute orientation error of four approaches, and list the results in Table I. We can see that, the fitting performance of PCA is very poor in terms of both metrics that it cannot meet the accuracy requirement of object detection in autonomous vehicle. Although the fitting results of L-shape fitting is much better than PCA, it still lower than the proposed rectangle fitting with aggregation criterion. Compared with L-shape fitting, the proposed rectangle fitting improves the mean of the two metrics by up to 0.07 and 3.52°, respectively. Moreover, the two metrics of the proposed aggregation criterion also outperforms variance criterion by up to 0.06 and 2.96°, respectively. This results further confirm the effectiveness of the proposed aggregation criterion.

TABLE I: Normalized Unoverlapped Area and Orientation Error Comparisons on Obstacle Detection

Method	Normalized Unoverlapped Area		Absolute Orientation Error	
	Mean	STD	Mean (deg)	STD (deg)
PCA [9]	0.82	1.19	26.61	12.47
L-shape [7]	0.21	0.19	8.05	9.91
Rec-var	0.19	0.16	7.48	9.90
Rec-CTAG	0.13	0.14	4.52	6.98

We also select all the vehicle clusters (104) in the dataset and evaluate the fitting performance of four different approaches on vehicle detection. The mean and standard deviation (STD) for the normalized unoverlapped area and absolute orientation error on vehicle detection is list in Table II. The evaluation results

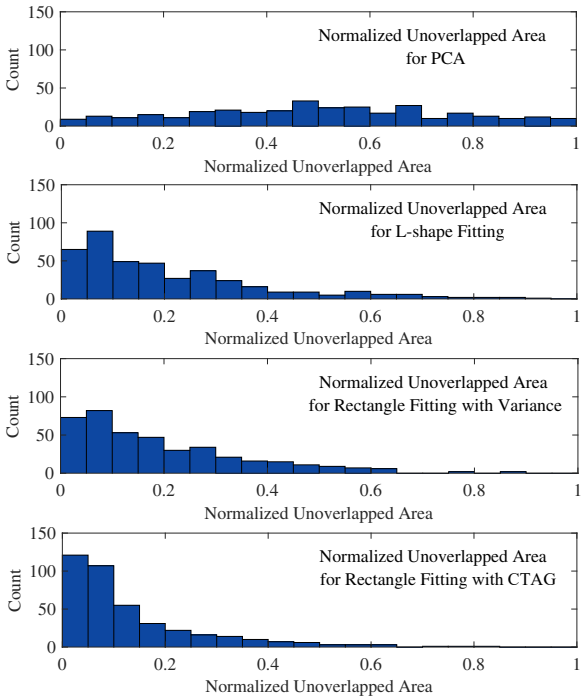

Fig. 8: Histogram of normalized unoverlapped area.

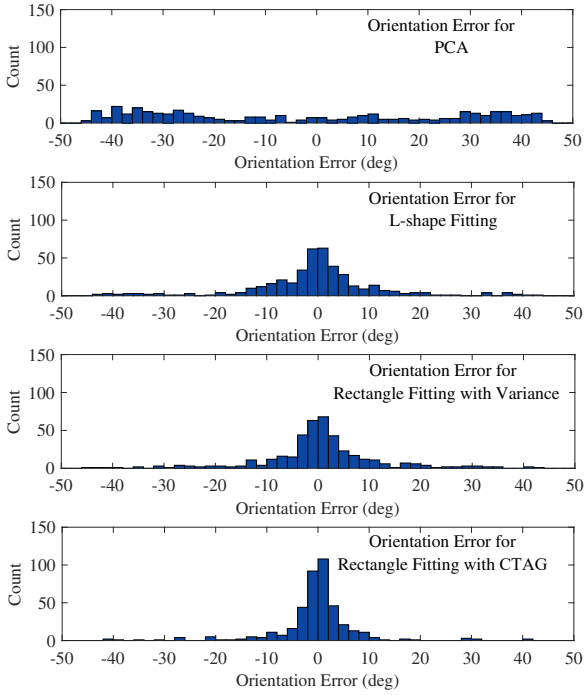

Fig. 9: Histogram of orientation error.

clearly show that the proposed rectangle fitting is also superior to vehicle detection, as there are many cases that the L-shape vehicle model assumption does not hold. Compared with L-shape fitting, the proposed rectangle fitting improves the mean of the normalized unoverlapped area and absolute orientation error by up to 0.03 and 0.98°, respectively.

TABLE II: Normalized Unoverlapped Area and Orientation Error Comparisons on Vehicle Detection

Method	Normalized Unoverlapped Area		Absolute Orientation Error	
	Mean	STD	Mean (deg)	STD (deg)
PCA [9]	0.65	0.35	30.30	9.46
L-shape [7]	0.10	0.12	3.01	3.82
Rec-var	0.09	0.09	2.79	3.05
Rec-CTAG	0.06	0.06	2.03	2.28

Fig. 10 shows an example of rectangle fitting for concave object. As we explained in the previous sections, the direct use of rectangle fitting to the concave object in Fig. 10 (a) will certainly incur serious issues that the majority area of rectangle bounding box is actually drivable region. In the proposed object detection approach, concave object is recognized by concavity determination, segmented into several clusters and then employed with rectangle fitting. Fig. 10 (b) shows that the proposed approach is effective to address the issue incurred by concave object.

Fig. 11 shows two examples of the proposed object

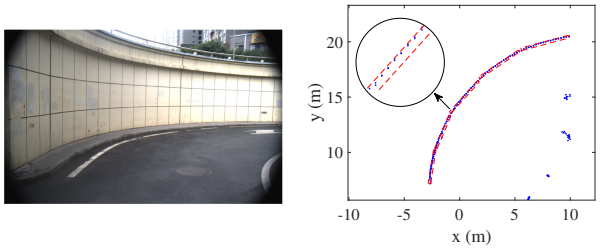

(a) (b)

Fig. 10: An example of rectangle fitting for concave object. The kmeans parameter k = 10 in our case.

detection and rectangle fitting results for typical laser scan cycles. The two examples are collected on the second ring road of Xi'an city, which is a complex urban traffic environment. The position of the 2D LIDAR is locate at coordinates (0, 0). Six cars scattered around in Fig. 11 (a) and four cars crossing the intersection in Fig. 11 (c) are well fitted in Fig. 11 (b) and (d) respectively.

C. Computational Efficiency

All the 110,000 clusters in the 40,000 laser scans are used to evaluate the computational efficiency of the three fitting approaches. The approaches are implemented with C++ language and run on a Windows industrial computer mounted in the trunk of "Discovery". The computer is equipped with an Intel Core i7 2.30GHz CPU and 4GB DRAM.

The average computation times of three fitting approaches for each cluster are illustrated in Table III. We can see that PCA [9] can run very fast that its average

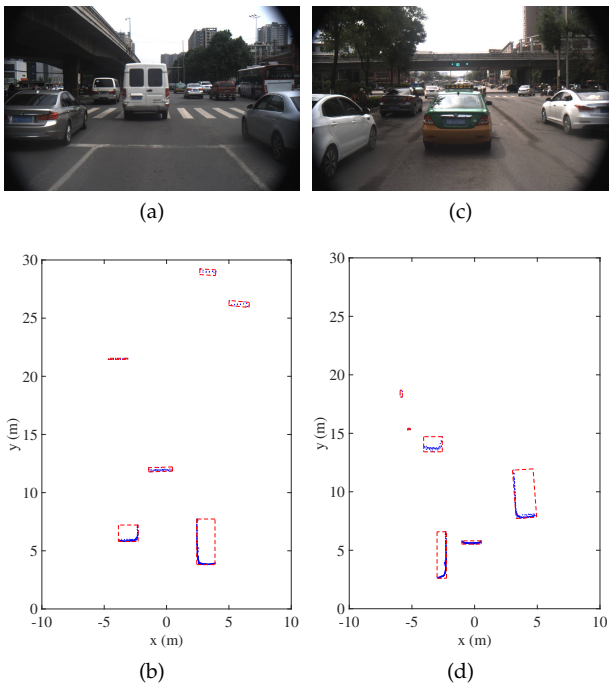

Fig. 11: Examples of proposed object detection and rectangle fitting results for typical laser scan cycles.

computation time is only 0.53 ms. However, its fitting performance is too poor to meet the accuracy requirement of autonomous vehicle. As the implementation of the proposed rectangle fitting eliminates the step of finding closer boundaries, while distance calculation is nearly the same, it can achieve higher efficiency than L-shape fitting. The average computation time of the proposed rectangle fitting is 32% lower than that of L-shape fitting. In addition, the computational efficiency of the overall object detection method is evaluated by using all the 40,000 laser scans. The processing performance on average can reach up to 20Hz (20 laser scans per second). Taking into consideration that the laser sensor works at the scan frequency of 6.25Hz, the proposed method can certainly meet the real-time requirement of object detection.

TABLE III: Computation Time Comparison

Method	Mean (ms)	STD (ms)
PCA [9]	0.53	0.12
L-shape [7]	13.49	5.75
Rectangle	9.06	3.49

V. Conclusion

This paper aims to exploit a robust and efficient on-road object detection method based on 2D LIDAR sensor. In particular, we propose a rectangle fitting approach to detect objects and estimate their orientation from sparse laser data. The proposed rectangle fitting can well address the issue incurred by concave object, and improve the robustness and efficiency of object detection by using rectangle model assumption and aggregation criterion. The proposed rectangle fitting approach is extensively evaluated on autonomous vehicle platform and realistic dataset. Experimental results demonstrate that the proposed rectangle fitting outperforms previous approaches in terms of both fitting performance and computational efficiency.

References

[1] Y. Zhang, J. Wang, X. Wang, C. Li, and L. Wang, "3d lidar-based intersection recognition and road boundary detection method for unmanned ground vehicle," in *IEEE International Conference on Intelligent Transportation Systems*, 2015, pp. 499–504.

[2] D. Zhao, Y. Yang, J. Huang, and Y. Liu, "Vehicle position estimation using geometric constants in traffic scene," in *IEEE International Conference on Service Operations and Logistics, and Informatics*, 2014, pp. 90–95.

[3] L. Chen, J. Yang, and H. Kong, "Lidar-histogram for fast road and obstacle detection," in *IEEE International Conference on Robotics and Automation*, 2017, pp. 1343–1348.

[4] T. Chen, B. Dai, D. Liu, H. Fu, J. Song, and C. Wei, "Likelihood-field-model-based vehicle pose estimation with velodyne," in *IEEE International Conference on Intelligent Transportation Systems*, 2015, pp. 296–302.

[5] S. Sivaraman and M. M. Trivedi, "Looking at vehicles on the road: A survey of vision-based vehicle detection, tracking, and behavior analysis," *IEEE Transactions on Intelligent Transportation Systems*, vol. 14, no. 4, pp. 1773–1795, 2013.

[6] X. Shen, S. Pendleton, and M. H. Ang, "Efficient L-shape fitting of laser scanner data for vehicle pose estimation," in *IEEE International Conference on Cybernetics and Intelligent Systems and IEEE Conference on Robotics, Automation and Mechatronics*, 2015, pp. 173–178.

[7] X. Zhang, W. Xu, C. Dong, and J. M. Dolan, "Efficient L-shape fitting for vehicle detection using laser scanners," in *IEEE Intelligent Vehicles Symposium*, 2017, pp. 54–59.

[8] R. MacLachlan and C. Mertz, "Tracking of moving objects from a moving vehicle using a scanning laser rangefinder," in *IEEE Intelligent Transportation Systems Conference*, 2006, pp. 301–306.

[9] H. Zhao, Q. Zhang, M. Chiba, R. Shibasaki, J. Cui, and H. Zha, "Moving object classification using horizontal laser scan data," in *IEEE International Conference on Robotics and Automation*, 2009, pp. 2424–2430.

[10] F. U. Siddiqui, S. W. Teng, G. Lu, and M. Awrangjeb, "An improved building detection in complex sites using the lidar height variation and point density," in *International Conference on Image and Vision Computing New Zealand*, 2013.

[11] M. Ester, H.-P. Kriegel, J. Sander, and X. Xu, "A density-based algorithm for discovering clusters in large spatial databases with noise," pp. 226–231, 1996.

[12] O. Khatib, "Real-time obstacle avoidance for manipulators and mobile robots," *The international journal of robotics research*, vol. 5, no. 1, pp. 90–98, 1986.